ADDING ENVIRONMENTAL GAS PHYSICS TO THE SEMI-ANALYTIC METHOD FOR GALAXY FORMATION: GRAVITATIONAL HEATING

Sadegh Khochfar
Department of Physics, University of Oxford and
Denys Wilkinson Bldg., Keble Road, Oxford, OX1 3RH, UK

and

Jeremiah P. Ostriker
Department of Astrophysical Sciences, Princeton University and
Peyton Hall, Princeton, NJ 08544, USA
accepted to ApJ

ABSTRACT

We present results of an attempt to include more detailed gas physics motivated from hydrodynamical simulations within semi-analytic models (SAM) of galaxy formation, focusing on the role that environmental effects play. The main difference to previous SAMs is that we include 'gravitational' heating of the intra-cluster medium (ICM) by the net surplus of gravitational potential energy released from gas that has been stripped from infalling satellites. Gravitational heating appears to be an efficient heating source able to prevent cooling in environments corresponding to dark matter halos more massive than $\sim 10^{13} M_\odot$. The energy release by gravitational heating can match that by AGN-feedback in massive galaxies and can exceed it in the most massive ones. However, there is a fundamental difference in the way the two processes operate. Gravitational heating becomes important at late times, when the peak activity of AGNs is already over, and it is very mass dependent. This mass dependency and time behaviour gives the right trend to recover down-sizing in the star-formation rate of massive galaxies. In general we find that environmental effects play the largest role in halos more massive than M^* at any given redshift because of the continued growth by mergers in these halos. We present a number of first order comparisons of our model to well established observations of galaxy properties which can be summarised as follows: The cosmic star formation rate can be reproduced with a decline at $z < 1$ that is steeper with respect to our SAM without environmental effects. The steep decline is mainly driven by a suppression of star formation in high density environments. In addition the star formation episode of our model galaxies is a strong function of mass. Massive galaxies with $M_* > 10^{11} M_\odot$ make most of their stars at look back times of roughly 11 Gyrs and show very low amounts of residual star formation at late times due to the suppression by environmental effects. In addition the luminosity function and colour bi-modality of the galaxy population are reproduced well.

Subject headings: galaxies: evolution — galaxies: formation — galaxies: general methods: numerical

1. INTRODUCTION

The simplest semi-analytic model (SAM) for galaxy formation might assume that the nature of a galaxy is determined solely by the mass and merging history of the dark matter halo or sub-halo within which it resides. But correlations between the observed properties of galaxies and their environments have been known for many years now. An increased fraction of early-type galaxies towards the centres of clusters (Dressler 1980; Dressler & Gunn 1982; Smith et al. 2005), or the increased fraction of blue, star forming galaxies in clusters at high redshift compared to their low redshift counter parts, the Butcher-Oemler effect (Butcher & Oemler 1978, 1984). Massive elliptical galaxies in clusters are on average older than comparable ellipticals in the field (Thomas et al. 2005) and the interaction rate of galaxies in clusters increases with redshift much more rapidly than in the field (van Dokkum et al. 1999) indicating accelerated galaxy transformation in dense environments. Recent studies of e.g. the Sloan Digital Sky Survey (SDSS) and the DEEP2 survey show that the fraction of galaxies of a given mass populating the red-sequence is a strong function of the environment (Baldry et al. 2006) and that indeed the environment can play an import role (Cooper et al. 2006) in driving galaxy evolution.

On the theoretical side first indictions for a possible transition in the mode of galaxy formation were found by Rees & Ostriker (1977), Silk (1977) and Binney (1977) who predicted a transition mass scale at which cooling times start becoming larger than the free-fall time. Differences arising from the environment are generally studied by assuming that the dark halo mass is a good proxy for the environment and that dark matter haloes greater than a few times $10^{14} M_\odot$ correspond to galaxy clusters (for a comparison between dark halo mass and galaxy surface density see Baldry et al. (2006)). Regarding the formation of dark matter halos and the mass assembly of galaxies, the CDM-paradigm predicts massive dark haloes to have a larger fraction of their final mass in progenitors at earlier times compared to low mass halos (e.g. Neistein et al. 2006) resulting in an increased merger fraction of galaxies at larger redshifts in high density environ-

Electronic address: sadeghk@astro.ox.ac.uk
Electronic address: ostriker@princeton.edu

ments (Khochfar & Burkert 2001). Furthermore, galaxies falling into dense environments are subject to interaction between the hot intra-cluster medium (ICM) and the inter-stellar medium (ISM) in form of ram-pressure stripping (Gunn & Gott 1972; Farouki & Shapiro 1980; Abadi et al. 1999; Mori & Burkert 2000) and shock heating (e.g. Frenk et al. 1999) that can allow for morphological transformation of galaxies by depriving them of gas (Quilis et al. 2000) and inducing star formation (Marcillac et al. 2007). The interplay between these processes will influence galaxies within a dark matter halo and should in a natural way account for many observations. Models based on a phenomenological approach to stop cooling flows in halos above a critical mass (e.g Kauffmann et al. 1999; Binney 2004) and hence in dense environments prove to be promising by being able to reproduce the luminosity function and colour bi-modality of the local galaxy population (e.g Cattaneo et al. 2006). Many of these effects are already seen in hydrodynamic simulations (Blanton et al. 1999, 2000).

The purpose of this paper is to illustrate the consequences that result from environmental effects usually omitted within semi-analytic models (SAM). These effects are real and automatically included in hydrodynamical simulations of sufficient resolution (see e.g. Naab et al. 2007), but we do not intend to claim that the implementation attempted in this paper is definitive or even, necessarily a substantial improvement over current modeling methods. Rather we intend to show the sign of the effects and the rough order of magnitude of the effects produced. In many cases these physical effects produce consequences that seem at variance (or even in some cases opposite) to overly naive interpretations of the hierarchical scenario that are consequent to gravitational interactions alone. Also, we wish to make clear at the outset that the physical effects described in this paper are independent of "feedback" which concept we define to be related to the return of energy, momentum and mass to the environment from evolving stars and central black holes. These feedback effects are also real, but they should not be confused with those gas physics effects that would necessarily occur even if there were neither stars nor AGNs. If the effects that we are adding to the SAM prescription are found to be useful, the correct way to implement them will be to use comparisons with detailed high resolution numerical hydro simulations, which are just now becoming available, and of course feedback effects from central black holes (Ciotti & Ostriker 2001; Springel et al. 2005; Croton et al. 2006; Bower et al. 2006; Kang et al. 2006; Ciotti & Ostriker 2007) must also be added to a comprehensive treatment for most accurate results.

We briefly summarise here the additional gas physics we have included to our basic model introduced in section 2 that made the most important differences in the model predictions, before we show later the details of the implementation (section 3) and first results (sections 4-8). For individual satellite galaxies we relaxed the generally applied assumption of instantaneous shock heating of hot gas in them when they fall into dense environments (Section 3.1) and added a prescription for ram-pressure stripping of gas (Section 3.2) while they orbit in a dense environment. We modify cooling flows for central galaxies, generally the most massive galaxies within a dark matter halo, by taking into account the heating of the ICM by gravitational heating from potential energy released by stripped gas from satellites (section 3.3). This additional energy source, which is not usually included in SAM treatments (but automatically allowed for in hydro treatments) adds energy to the gas in amounts comparable to the energy added by feedback processes.

2. THE SEMI-ANALYTIC MODEL

The main strategy behind the modelling approach we follow is first to calculate the collapse and merging history of individual dark matter halos, which is governed purely by gravitational interactions, and secondly to estimate the more complex physics of the baryons inside these dark matter halos, including e.g. radiative cooling of the gas, star formation, and feedback from supernovae by simplified prescriptions on top of the dark matter evolution (e.g. Silk 1977; White & Rees 1978; White & Frenk 1991; Kauffmann et al. 1999; Somerville & Primack 1999; Cole et al. 2000; Hatton et al. 2003; Cattaneo et al. 2006; Croton et al. 2006; Bower et al. 2006; De Lucia & Blaizot 2007). Each of the dark matter halos will consist of three main components which are distributed among individual galaxies inside them: a stellar, a cold, and a hot gas component, where the latter is only attributed to *central* galaxies, which are the most massive galaxies inside individual halos and typically are observed to reside in extended X-ray emitting coronal gas. In the following sections, we will describe briefly the recipes used to calculate these different components which are mainly based on recipes presented in e.g. Kauffmann et al. (1999) (hereafter, K99), Cole et al. (2000) (hereafter, C00) and Springel et al. (2001) (hereafter, S01), and we refer readers for more details on the basic model implementations to their work and references therein. In the remainder of this paper we call the *standard/old* SAM the model implementation presented in Khochfar & Burkert (2003, 2005) which is summarized in this section. The new additional environmental physics is presented in section 3. Throughout this paper we use the following set of cosmological parameters motivated by the 3 year results of WMAP (Spergel et al. 2007): $\Omega_0 = 0.27$, $\Omega_\Lambda = 0.73$, $\Omega_b/\Omega_0 = 0.17$, $\sigma_8 = 0.77$ and $h = 0.71$.

2.1. *Dark Matter Evolution*

We calculate the merging history of dark matter halos according to the prescription presented in Somerville & Kolatt (1999). This approach has been shown to produce merging histories and progenitor distributions in reasonable agreement with results from N-body simulations of cold dark matter structure formation in a cosmological context (Somerville et al. 2000). The merging history of dark matter halos is reconstructed by breaking each halo up into progenitors above a limiting minimum progenitor mass M_{min}. This mass cut needs to be chosen carefully as it ensures that the right galaxy population and merging histories are produced within the model. Progenitor halos with masses below M_{min} are declared as *accretion* events and their histories are not followed further back in time. Progenitors labelled as accretion events should ideally not host any significant galaxies in them and be composed mainly of primordial hot gas at the progenitor halo's virial temperature.

The mass scale at which this is the case can in principle be estimated from the prescriptions of supernova feedback and reionisation presented in section 2.2.1. However, to achieve a good compromise between accuracy and computational time, we instead estimated M_{min} by running several simulations with different resolutions and chose the resolution for which results in the galaxy mass range of interest are independent of the specific choice of M_{min}. Changing the mass resolution mainly affects our results at low galaxy mass scales, leaving massive galaxies nearly unaffected. Throughout this paper we will use $M_{min} = 10^{10}$ M$_\odot$ which produces numerically stable results for galaxies with stellar masses greater a few times 10^{10} M$_\odot$.

2.2. Baryonic Physics

As mentioned above, once the merging history of the dark matter component has been calculated, it is possible to follow the evolution of the baryonic content in these halos forward in time. We assume each halo consists of three components: hot gas, cold gas and stars, where the latter two components can be distributed among individual galaxies inside a single dark matter halo. The stellar components of each galaxy are additionally divided into bulge and disc, to allow morphological classifications of model galaxies. In the following, we describe how the evolution of each component is calculated.

2.2.1. Gas Cooling & Reionisation

Each branch of the merger tree starts at a progenitor mass of M_{min} and ends at a redshift of $z = 0$. Initially, each halo is occupied by hot primordial gas which was captured in the potential well of the halo and shock heated to its virial temperature $T_{vir} = 35.9 \left[V_c / (\text{km s}^{-1}) \right]^2$ K, where V_c is the circular velocity of the halo (White & Frenk 1991, K99). Subsequently this hot gas component is allowed to radiatively cool and settles down into a rotationally supported gas disc at the centre of the halo, which we identify as the central galaxy (e.g Silk 1977; White & Rees 1978; White & Frenk 1991). The rate at which hot gas cools down is estimated by calculating the cooling radius inside the halo using the cooling functions provided by Sutherland & Dopita (1993) and the prescription in S01. In the case of a merger between halos we assume that all of the hot gas present in the progenitors is shock heated to the virial temperature of the remnant halo (in our new model including environmental effects we will relax this assumption, see 3.1), and that gas can only cool down onto the new central galaxy which is the central galaxy of the most massive progenitor halo. The central galaxy of the less massive halo will become a satellite galaxy orbiting inside the remnant halo. In this way, a halo can host multiple satellite galaxies, depending on the merging history of the halo, but will always only host one central galaxy onto which gas can cool. The cold gas content in satellite galaxies is given by the amount present when they first became satellite galaxies and does not increase (this will again will be modified in our new environmental prescription, see 3.1, instead it decreases due to ongoing star formation and supernova feedback.

In the simplified picture adopted above, the amount of gas available to cool down is only limited by the

universal baryon fraction $\Omega_b h^2 = 0.023$ (Spergel et al. 2007). However, in the presence of a photoionising background the fraction of baryons captured in halos is reduced (e.g. Gnedin 2000; Benson et al. 2002) and we use the recipe of Somerville (2002), which is based on a fitting formulae derived from hydrodynamical simulations by Gnedin (2000), to estimate the amount of baryons in each halo. For the epoch of reionisation, we assume $z_{reion} = 7$, which is in agreement with observations of the temperature-polarisation correlation of the cosmic microwave background by Spergel et al. (2007).

2.2.2. Star formation in Discs and Supernova Feedback

Once cooled gas has settled down in a disc, we allow for fragmentation and subsequent star formation according to a parameterised global Schmidt-Kennicutt type law (Kennicutt 1998) of the form $\dot{M}_* = \alpha M_{cold}/t_{dyn,gal}$, where α is a free parameter describing the efficiency of the conversion of cold gas into stars, and $t_{dyn,gal}$ is assumed to be the dynamical time of the galaxy and is approximated to be $1/40$ times the dynamical time of the dark matter halo (Naab & Ostriker 2006).

Feedback from supernovae plays an important role in regulating star formation in small mass halos and in preventing too massive satellite galaxies from forming (Dekel & Silk 1986). We implement feedback based on the prescription presented in K99 with

$$\Delta M_{reheat} = \frac{4}{3} \epsilon \frac{\eta_{SN} E_{SN}}{V_c^2} \Delta M_*. \tag{1}$$

Here we introduce a second free parameter ϵ which represents our lack of knowledge on the efficiency with which the energy from supernovae reheats the cold gas. The expected number of supernovae per solar mass of stars formed for a typical IMF is $\eta_{SN} = 5 \times 10^{-3}$, and $E_{SN} = 10^{51}$ erg is the energy output from each supernova. We take V_c as the circular velocity of the halo in which the galaxy was last present as a central galaxy.

2.2.3. Galaxy Mergers

We allow for mergers between galaxies residing in a single halo. As mentioned earlier, each halo is occupied by one central galaxy and a number of satellite galaxies depending on the past merging history of the halo. Whenever two halos merge, the galaxies inside them will merge on a time-scale which we calculate by estimating the time it would take the satellite to reach the centre of the halo under the effects of dynamical friction. Satellites are assumed to merge only with central galaxies and we set up their orbits in the halo according to the prescription of K99, modified to use the Coulomb logarithm approximation of S01.

If the mass ratio between the two merging galaxies is $M_{gal,1}/M_{gal,2} \leq 3.5$ ($M_{gal,1} \geq M_{gal,2}$) we declare the event as a *major* merger and the remnant will be an elliptical galaxy. We assume that the stellar components of the progenitors add up to form a spheroid, that the cold gas present in the progenitors ignites in a central star burst, and that the hot gas components add up. In the case of a *minor* merger $M_{gal,1}/M_{gal,2} > 3.5$, we assume that the stellar component of the smaller progenitor adds to the bulge of the larger progenitor and that the cold gas in the disc of the smaler progenitor settles down into the disc of the larger progenitor.

3. ENVIRONMENTAL EFFECTS

The basic model introduced in the previous section already includes several environmental dependencies as e.g. the merger rate of galaxies increase more steeply with redshift in high density environments like clusters (Khochfar & Burkert 2001), a feature also seen in observations (van Dokkum et al. 1999). In this section we intend to incorporate further physical effects that are important to model the evolution of the galaxy population and that are already self-consistently included in hydrodynamical simulations (e.g. Frenk et al. 1999). Of these effects some were already implemented in similar ways in previous models by other authors, like e.g. ram-pressure stripping and shock heating (e.g. Lanzoni et al. 2005). Some of the effects of gravitationl heating have been discussed recently by Wang & Abel (2007) but have not yet been implemented within the context of a SAM.

The main difference to the SAM implementation of the previous section is that we here follow explicitly the heating of the hot gas phase by the conversion of gravitational potential energy. To avoid adding liberated energy twice to the hot gas phase we adopt the following prescription. Initially, when the dark matter halo becomes more massive than M_{min}, we set the temperature of the hot gas to T_{vir}. During the subsequent growth of the dark matter halo however, we do not automatically increase the temperature of the hot gas in the host to the new virial temperature of the host dark matter halo (by host dark matter halo we always refer to the dark matter halo mass including all sub-structure). Instead we let it only increase by the energy gained from the potential energy of the gas that is stripped from the substructure (see parargraph 3.3 and 3.4). At each step in our simulation we keep track of the specific energy of the hot gas component and thus are able to calculate its temperature T_{gas}. This allows us to define the parameter $f_e = 1 + (T_{vir} - T_{gas})/T_{vir}$ to calculate the energy needed to remove gas from a halo. We here assume that the cold gas phase has $T_{gas} = 0$ which sets $f_e = 2$ for cold gas and $f_e = 1$ for gas at the virial temperature of the halo. In general the liberated potential energy is sufficient to raise the temperature of the hot gas to the new virial temprature on a short time scale. Another main difference to the old SAM is that we allow satellites to have hot gas which is able to cool following the prescription in 2.2.1 and to subsequently form stars in the disk of the satellite galaxy. We remove hot gas from the satellites using the prescriptions laid out in sections 3.1 & 3.2.

The following sections are structured as follows, first we introduce our prescriptions for the stripping of gas from orbiting satellites by ram pressure and shock heating. This is necessary to help us approximate the rate at which potential energy is relased at each individual time step within our simulation. In the following two sections we then introduce the actual prescriptions for gravitational heating and its implemetation within our SAM.

3.1. Shock-heating of Gas

During the infall of satellite galaxies into dense environments, shock heating of satellite gas is occurring with the gas being removed from the satellite on time scales much shorter than the Hubble time (e.g.

Metzler & Evrard 1994; Frenk et al. 1999). Generally this process is implemented within SAMs by assuming that it is very efficient and quasi-instantaneous, thus depriving satellite galaxies of any reservoir of hot virialized gas (e.g. WF91, K99, C00). In the following we will relax this assumption and investigate its effects on the galaxy population.

Gas removal from the satellite occurs efficiently when the shock is depositing enough energy to heat the gas in the satellite above its virial temperature (e.g Metzler & Evrard 1994; Birnboim & Dekel 2003). This condition can be expressed in terms of the adiabatic sound speed in the host halo, $c_{\text{gas}}^2 = \gamma V_{max}^2/\beta$ with $\gamma = 5/3$ and $\beta \sim 1.25$ (Bryan & Norman 1998), and the satellite's maximum circular velocity $V_{max,sat}$ as

$$c_{\text{gas}}^2 \geq \zeta V_{\text{max,sat}}^2. \tag{2}$$

Here we introduce a free model parameter ζ which in effect regulates at which mass ratio, between infalling satellite and host halo, shock heating will occur. As we will show below the specific choice of ζ does not change the properties of the overall galaxy population significantly and only has influence on satellite galaxies. The gas fraction of galaxies within clusters is an increasing function of radius (Dressler 1986) supporting the assumption that whatever reduces the gas fraction must work on a time scale comparable to the dynamical time within the cluster. Once the condition in Eq. 2 is satisfied, we therefore allow for gas removal from the satellite on some fraction $1/\delta$ of the host halo's dynamical time. In general we find that the gas in our simulations will be completely shock heated on time scales less than a Gyr with a tendency for faster heating in low mass satellites as shown by the conditional probability distribution $p(t_{dyn}|M_{hot})$ of infalling satellite galaxies in Fig. 1.

Shocks will not only heat the hot gas phase, but also penetrate deep within the satellite and heat the cold gas phase (T. Naab, private communication). We include this effect, sometimes neglected within SAMs, in the same manner as described above. In consequence at each time step within the simulation we have the following mass loss from each satellite due to shock heating which will be added to the hot gas content of the host central galaxy:

$$\frac{dM_{\text{hot,sat}}}{dt} = -\delta \frac{M_{\text{hot,sat}}}{t_{dyn,halo}} \tag{3}$$

$$\frac{dM_{\text{cold,sat}}}{dt} = -\delta \frac{M_{\text{cold,sat}}}{t_{dyn,halo}}. \tag{4}$$

A first comparison between our initial model (labelled 'old SAM'), including instantaneous shock heating of only hot gas, in Fig. 2 does not show any significant difference in the cold and hot gas mass function of central galaxies. On the contrary Fig. 3 shows that satellites tend to retain more cold and hot gas when the condition for shock heating, as laid out by Eq. 2, requires them to fall into a much more massive host (larger ζ) and if the time scale for shock heating is longer (smaller δ). In all cases the amount of gas shock heated is negligible as compared to the hot gas content of the host central galaxy, explaining the lack of change in the gas mass function. The overall galaxy population at the intermediate to massive end is dominated by central galaxies
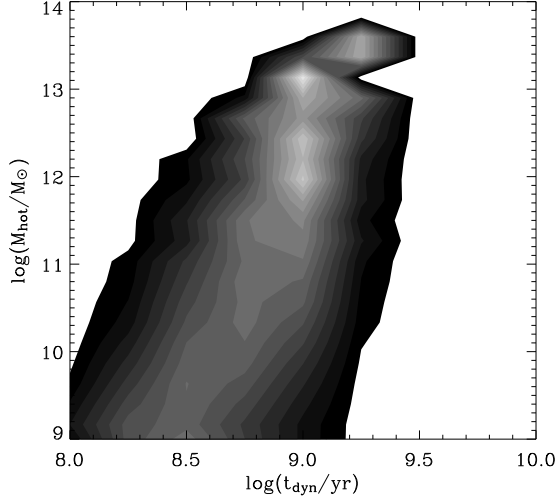
FIG. 1.— Conditional probability contours $p(t_{dyn}|M_{hot})$ of satellite galaxies when they enter the host dark matter halo. The dynamical time t_{dyn} has been calculated for the host dark matter halo and M_{hot} is the amount of hot gas within the satellite galaxy.

which are unaffected by the specific choices of the shock heating parameters and we choose to omit these parameters for the remainder of this paper, i.e. set them to $\zeta = 1$ and $\delta = 1$.

3.2. Ram Pressure Stripping

Individual late-type galaxies within clusters show perturbed HI disks which are reduced in size with respect to their stellar disks (for a review see van Gorkom 2004) and are HI deficient with respect to field late type galaxies, a fact generally attributed to ram pressure stripping caused by the interactions between the hot ICM and the ISM of the satellite (Gunn & Gott 1972; Giovanelli & Haynes 1983; Quilis et al. 2000). The time scale for this process must be less than 1 Gyr as indicated by the abrupt truncation of star formation in passive cluster spirals (Moran et al. 2006). However, it is very likely that ram pressure stripping alone is not sufficient to cause the observed HI deficit in satellite galaxies Abadi et al. (1999) and that other processes like e.g. shock heating play an important role. Furthermore, SAMs including ram pressure stripping alone, only report negligible changes in galaxy properties like colours and star formation rates (Okamoto & Nagashima 2003; Lanzoni et al. 2005).

Following Gunn & Gott (1972) we assume that gas is stripped from the satellite once the dynamical pressure is able to overcome the gravitational force binding the gas to the satellite. In terms of energy deposited within the satellite gas this can be approximated by:

$$\dot{E}_{ram} = \mu \rho_{hot} v_\perp^3 \pi r_h^2. \tag{5}$$

Here we take $v_\perp$ as the velocity of the satellite perpendicular to its disk orientation and assume that the orbital velocity of the satellite is comparable to the sound speed c_{gas} of the hot gas. The efficiency of this process for a face-on disk should be maximal and minimal for an edge-on disk and we take this into account by assuming the disk orientation is random with respect to the infall direction. This is in good agreement with cosmological dark matter simulations which show that the spin vector of merging dark matter halos are randomly aligned
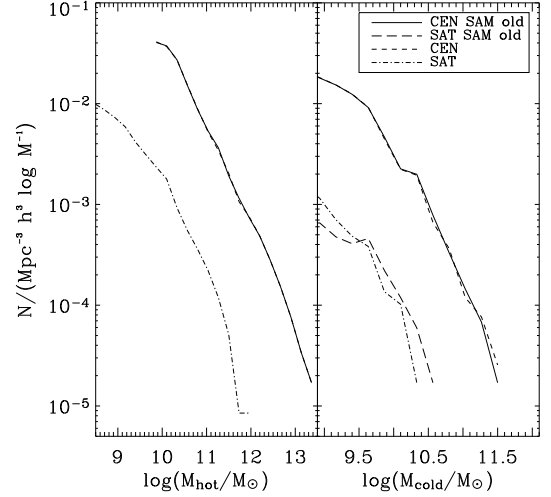

FIG. 2.— Hot and cold gas mass function for satellite (SAT) and central galaxies (CEN) in the model including shock heating of hot and cold satellite gas. The initial semi-analytic model without environmental effects is labelled 'SAM old'. Please note that the initial SAM by construction does not have any satellite galaxies with hot gas reservoirs because we assume instantaneous heating of it.

to each other (Khochfar & Burkert 2006). We assign a random angle $\alpha_\perp$ between the disk plane and the velocity vector of the satellite and calculate $v_\perp$ by $c_{gas} \sin \alpha_\perp$ (Lanzoni et al. 2005). For simplicity we calculate the density ρ_{hot} by taking the average density of hot gas within the host halo's virial radius and take r_h to be the characteristic half mass radius of the gas within the satellite. We introduce a free parameter μ which allows us to investigate the importance of this process. As we will show below, the efficiency parameter μ does not influence general galaxy properties significantly. Equation 5 is an upper limit to the expected ram pressure heating of the gas in the satellite as we neglect tidal stripping and the change in the velocity of the satellite while it orbits through the host halo (see e.g. Taylor & Babul 2001).

The amount of cold disk gas stripped from the satellite can be calculated by:

$$\frac{dM_{ram,c}}{dt} = -\frac{4}{3} \frac{\dot{E}_{ram,c}}{f_e V_{max,sat}^2}. \tag{6}$$

Here we use in Eq. 5 the observed mean size-mass relation reported for disk galaxies from the SDDS (Shen et al. 2003). We note that this might be an overestimate as disk galaxies tend to be smaller by a factor of up to 1.5 at $z = 2.5$ (Trujillo et al. 2005).

$$\frac{dM_{ram,h}}{dt} = -\frac{4}{3} \frac{\dot{E}_{ram,h}}{f_e V_{max,sat}^2}. \tag{7}$$

Not only cold gas in disks is subject to ram pressure stripping but also diffuse hot halo gas (e.g. Machacek et al. 2006) and we model this process in the same way as for the cold gas case with the exception that $r_h = r_{vir,sat}/2$ in Eq. 5 and that the energy needed to heat a unit mass to the virial temperature of the host halo is less since the hot gas in the satellite is already at some temperature T_{gas}. The hot gas mass stripped from the satellite is

The rate at which material is stripped in our implementation of ram pressure varies from earlier approaches.
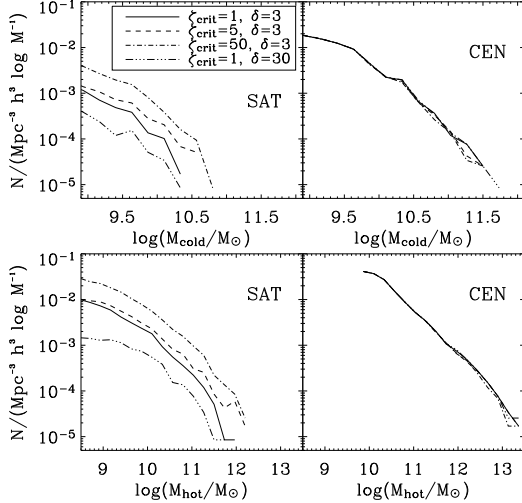
FIG. 3.— Hot and cold gas mass functions for different choices of parameters in the shock heating model. We omit showing the initial SAM because it is almost identical to the model with $\delta = 3$ and $\zeta = 1$.

E.g. Okamoto & Nagashima (2003) assume instantaneous stripping of all gas once the ram pressure overcomes a characteristic restoring force per unit area in the galactic disk, calculated using the surface mass density at the half mass radius. Other implementations have a more gradual stripping rate, assuming an exponential profile for the surface mass density of material in the satellite disk (Lanzoni et al. 2005). Common to both of these implementations is that they assume a radial profile for the gas density in the host halo and that the time dependence of the stripping is driven basicly by the physical location of the satellite within the halo. In our implementation the time dependency is due to the continued transfer of energy to the gaseous disk of the satellite. For a host halo that is not significantly changing its average gas density with time, we deposit a constant amount of energy per unit time within the gaseous disk of the satellite. The stripping rate we calculate in this way is initially larger than that from gradual models like the one of Lanzoni et al. (2005). Such models however predict an increase in the stripping rate with time, due to the increasing ambient gas density while the satellite orbits towards the centre of the host halo. The effect of these different implementations on the galaxy populations is very mild. In our model the cold and hot gas mass function of central galaxies are mostly unaffected by ram pressure stripping from satellite galaxies in comparison to our initial SAM shown in the upper panel of Fig. 4 and in agreement with previous work (Okamoto & Nagashima 2003; Lanzoni et al. 2005). The reason we do not find significant changes in the overall galaxy population is that central galaxies dominate the mass range studied here and that the gas fraction of satellites is much less than that of centrals. Increasing the efficiency μ by two orders of magnitude only marginally reduces the amount of hot and cold gas in satellites. Therefore again we omit using this free parameter, i.e. set it to $\mu = 1$.

3.3. *Gravitational Heating*

The energy used to expel gas from satellites is contributed from the gravitational potential energy that is gained when a satellite becomes bound in the potential of
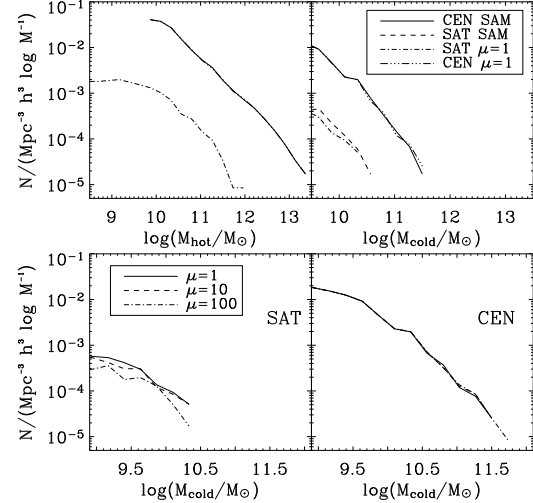

FIG. 4.— Same as Fig. 3, but in this simulation we only included ram pressure stripping of satellite gas with different stripping efficiencies μ.

the primary halo. The majority of dark halos are initially on parabolic orbits with $E_{tot} = 0$ (Khochfar & Burkert 2006) before they become bound and merge. According to the virial theorem, maximally half of the potential energy gained could be used to heat the ICM. We here take into account the energy gained by each infalling mass unit of gas and subtract from it the energy necessary to expel it from the potential of the satellite and to heat it to the virial temperature of the host.

The rate at which energy is gained is connected to the rate at which gas is expelled from satellites $\dot{m}_{gas}$, according to the prescriptions in section 3.1 & 3.2. At each time step within our simulation we calculate:

$$\dot{E}_{grav} = \sum_{i=1,n_{sat}} \dot{m}_{gas,i} \left[\Delta\phi - b\frac{3}{4}V_{max,sat,i}^2 - \frac{3}{4}V_{max,cen}^2 \right] \tag{8}$$

where $b = 2$ for cold gas and $b = f_e$ for hot gas that is stripped from the satellites. Please note that Eq. 8 is the actual surplus of energy available to heat the ICM once the stripped gas of the satellite is heated to the virial temperature of the host. We model the dark matter halo of the host as a truncated isothermal sphere with core radius r_0 and calculate the amount of potential energy gained by the satellite when it reaches the virial radius $r_{vir,cen}$ of the host halo. For the halo we assume a characteristic value $r_{vir,cen}/r_0 = 25$ (Shapiro et al. 1999; Mayer et al. 2002). It should be noted that in general the concentration of dark matter halos is a function of mass and redshift (e.g. Bullock et al. 2001; Dolag et al. 2004) and that we ommit this dependency for the sake of simplicity at this stage. The gain in potential energy is then calculated as $\Delta\phi = -\ln(r_{vir,cen}/r_0)$. Within the simulation we will use the energy surplus calculated from Eq. 8 to heat and to counter cooling within the hot gas of the host halo. Eq. 8 is generally not included in SAMs, although it appears to be necessary in order to conserve energy.

The time integral of Eq. 8 can be quite substantial and, if expressed in terms of $E_{grav,tot} = \epsilon_{grav}m_*c^2$, we find values in Fig. 5 for ϵ_{grav} ranging from a few times 10^{-8} to a few times 10^{-4} in galaxies of $\sim 10^{10}$ and $\sim 5 \times 10^{12}$ $M_\odot$, respectively. That this increase is driven by the en-
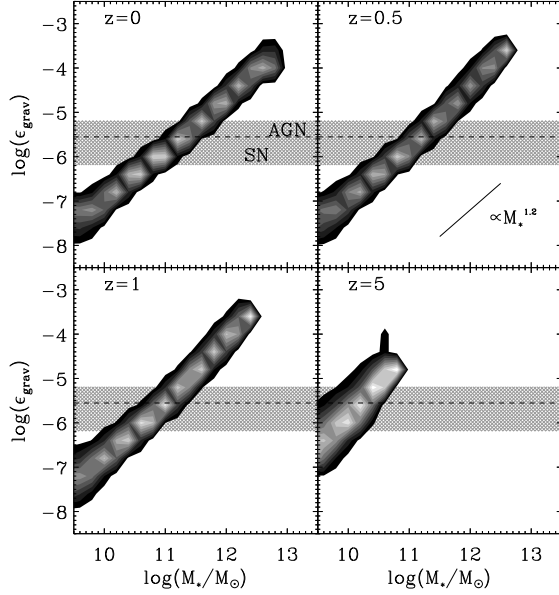
FIG. 5.— The gravitational heating efficiency ϵ_{grav} as a function of stellar mass for different redshifts. The crosshatched region shows the region were AGN and supernovae feedback operate. Estimates for supernovae feedback limit it mainly to below the dashed line, while estimates for AGN-feedback cover the whole region. The solid line shows a fit of the form $\propto M_*^{1.2}$.
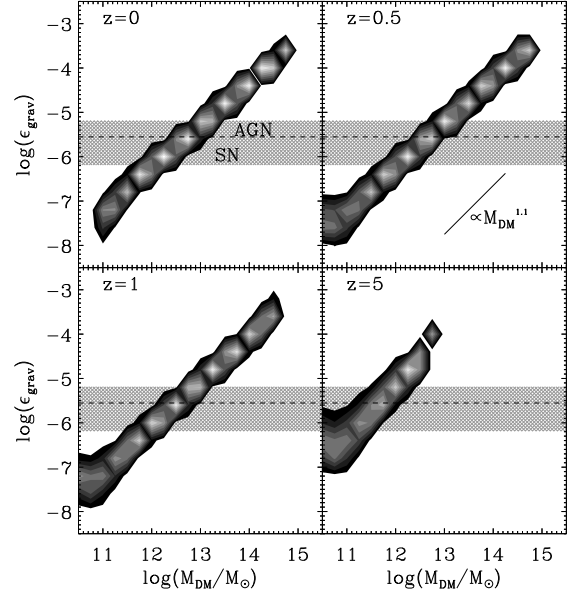
FIG. 6.— The gravitational heating efficiency ϵ_{grav} as a function of dark halo mass for different redshifts. Please note that at $z = 0$ the contours start at 10^{11} M$_\odot$ because we sample the mass function only between $10^{11} - 10^{15}$ M$_\odot$. The crosshatched region and dashed line indicate the regions of AGN and supernovae feedback as in Fig. 5. The solid line shows a fit of the form $\propto M_{DM}^{1.1}$. this fit is somewhat steeper than what would be expected from simple scaling arguments and indicates that in massive halos the ratio of expelled satellite gas to stellar mass of the central galaxy scales as $M_{DM}^{0.43}$.

vironment becomes most evident when considering the dependence of ϵ_{grav} on the dark matter halo mass in Fig. 6. Above a halo mass of 10^{11} M$_\odot$ ϵ_{grav} increases steadily. However, it appears that this increase is steeper at larger redshifts. We find that the upper limit for ϵ_{grav} lies around $\sim 5 \times 10^{-4}$ and that in general the most massive halos present at a given redshift tend to take on this values. One can understand this behaviour by considering the accretion of satellites onto halos. In general the most massive halos at any redshift have had the largest accretion rates in the past which explains the large amount of gravitational heating.

It is worth comparing gravitational heating to other common heating mechanisms like supernovae and AGN. Comparing ϵ_{grav} to $\epsilon_{SN} \sim 2.8 \times 10^{-6}$ and ϵ_{BH} with values between$\sim 6.5 \times 10^{-6}$ (Springel et al. 2005) and $\sim 6.5 \times 10^{-7}$ (Ciotti & Ostriker 2007) shows that in general gravitational heating is more efficient than supernovae feedback only in galaxies larger than a few times 10^{11} M$_\odot$ and in halos more massive than 5×10^{12} M$_\odot$ at $z = 0$. This regime correspond to massive field galaxies and extends into group like environments. For even more massive galxies and dark halo masses larger than 10^{13} M$_\odot$ gravitational heating starts dominating over proposed AGN-feedback rates. This is very interesting as one is dealing with mostly rich group and cluster environments which are subject to a very substantial gravitational heating generally neglected within SAMs. Furthermore, the most massive galaxies will have another large source of heating in addition to AGN-feedback that will prevent ongoing star formation and will naturally reduce the overproduction of galaxies at the bright end of the luminosity function (Benson et al. 2003). Again it is important to understand at which mass scales gravitational feedback operates at different times. At large redshifts it will become more important than supernovae

and AGN-feedback already in smaller halos and galaxies. As a consequence gravitational feedback can match AGN-feedback at the epoch of peak QSO-activity in the most massive halos and galaxies.

When considering the mass dependence of ϵ_{grav} we find over a wide range of masses roughly a $\propto M_{DM}^{1.1}$ dependency. It is worth noting that from simple scaling arguments one would expect that $\epsilon_{grav} \propto M_{DM}^{2/3} m_{gas}/m_*$, with m_{gas} as the total amount of gas expelled from satellite galaxies, indicating that the fraction of expelled gas to stellar mass of central galaxies scales as $\propto M_{DM}^{0.43}$. Going to smaller masses there is a distinctive break at a stellar mass of a few times 10^{10} M$_\odot$, which coincides with the break in properties of the galaxy population that is found in the Sloan Digital Sky Survey (Kauffmann et al. 2003). Our results suggest that this break could be the consequence of the accretion rate and hence the amount of gravitational energy that is released.

3.4. Implementation

At the beginning of our merger tree, i.e. when the dark matter halo first crosses M_{min} we set the temperature of the hot gas to the virial temperature T_{vir} of that halo and allow it to cool as described in 2.2.1. Once satellites fall onto the main halo, we calculate the amount of gas stripped from each individual orbiting satellite $\dot{m}_{gas}$ using Eqs. 2, 3, 5 & 7 plus the contribution from gas that leaves the satellite halo because of supernovae feedback. This $\dot{m}_{gas}$ is then used in Eq. 8 to calculate the amount of gravitational heating energy added to the ICM. Please not that in practice we use Eq. 8 without the last term $3/4 V_{max,cen}^2$, because the hot gas of the host might not be at T_{vir}, but at some lower temperature T_{gas}, and there-
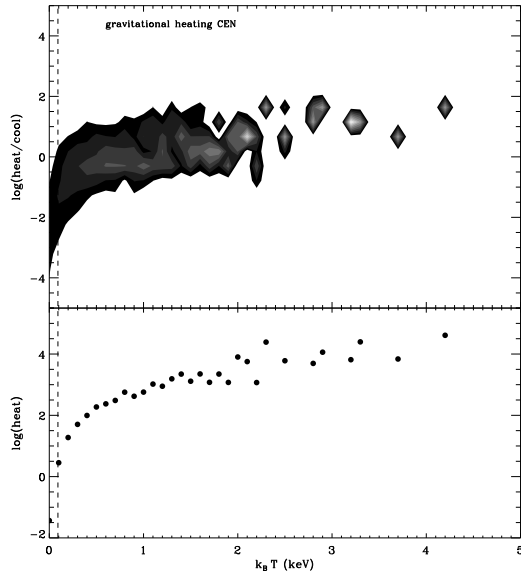
FIG. 7.— Contours of the effective heating-to-cooling rate $p(\log(heat/cool)|k_BT)$ at $z = 0.1$ as a function of the environment. We refer with *heat* to the amount of cold gas in $M_\odot$/yr that can be heated to the virial temperature of a galaxie's dark matter halo by gravitational potential energy released, and with *cool* to the amount of radiative cooling in $M_\odot$/yr that occurs at the same time. In effect the cold gas reservoir of a galaxy stays constant if $\log(heat/cool) = 0$. The top panel shows the heating-to-cooling rate of gas in central galaxies and the small panel on the bottom of each graph shows the absolute amount of heating in units of $M_\odot$/yr. The environment is indicated by the virial temperature of the dark matter halo associated with the central galaxy. The vertical dahed line in each graph shows the mass resolution of our simulation.

for the stripped gas will not automatically be heated to T_{vir} as assumed in Eq. 8. The energy contribtuion we calculated in this way is then used to heat the host hot gas to T_{vir}. If the gas is allready at T_{vir} or if energy is left after elevating it to T_{vir} we allow the surplus of energy to be used to counter the energy losses due to our cooling prescription in 2.2.1 and to reduce the amount of cooling gas. If there is still energy left after countering all the energy losses due to cooling we use it to increase the energy of the host hot gas. We here do not take into account the possiblility of gas leaving the host halo and getting lost once its energy gets to large to be bound, but instead assume it is marginally bound in a hot athmosphere. If two host halos merge we assume that the smaller one becomes a satellite and calculate f_e according to its specific energy and use it in Eqs. 2, 3, 5 & 7. The satellites within this halo will now be considered satellites of the new host halo and contribute their potential energy to the new host.

4. GENERAL RESULTS

To illustrate the contribution from gravitational heating we display the contours of the conditional probability for the ratio of heating to cooling that individual galaxies experience in a given environment. The top panel in Fig. 7 shows the probability contours for central galaxies at $z = 0.1$ in our simulaitons. We translate the deposited energy per unit time into a heating rate, labeled *heat* in Fig. 7, by calculating the amount of cold gas that can be heated to the virial temperature of the dark matter halo the galaxy resides in. The cooling rate for central

galaxies is calculated using the prescription outlined in section 2.2.1 and is labeled *cool* in Fig. 7.

The left panel shows the contribution from gravitational heating to the hot gas of central galaxies as gas gets stripped from satellites. The heating rate for the central galaxies is up to 10^2 times larger than the cooling rate and in the most dense environments the heating rate becomes 10^4 $M_\odot$ yr^{-1}. The heating rate shows a clear environmental dependence reflecting the higher abundance of satellites which contribute to gravitational heating. From these results one expects that star formation will be terminated in central galaxies of dense environments.

The importance of several physical processes depending on environment and redshift is shown in Fig. 8. The top left panel shows the average cooling rate in systems for which the cooling time is shorter than the dynamical time of the halo. This 'cold accretion' mode occurs in halos with masses below $\sim 10^{11} - 10^{12}$ $M_\odot$ and is most efficient at high redshifts in agreement with SPH-simulations by Kereš et al. (2005) and earlier analytic calculations (Binney 1977; Silk 1977; Rees & Ostriker 1977). The solid line in the same figure is the maximum halo mass which shows cold accretion at each redshift. The average amount of cold gas in the ISM reheated by supernovae is shown in the right top panel. Supernovae are able to heat gas efficiently in small halos with masses below $\sim 10^{12}$ $M_\odot$ and are responsible for shaping the low mass tail of the luminosity function (Dekel & Silk 1986). The results in the two top panels are usually incorporated in all semi-analytic models. The additional physics we included is shown in the lower panel of the same figure. It appears that the heating rate of the ICM by gravitational heating is always very efficient in the most massive halos one finds at each redshift, with several thousand solar masses per year, and not very efficient in low mass halos. This is not too surprising considering that low mass halos do have less infalling sub-sructure than cluster sized halos.

To illustrate how the new environmental effect operates we followed the $\epsilon-$'trajectory' of a random central and satellite galaxy back in time. This trajectory is calculated as in Khochfar & Silk (2006a,b) by summing up the ϵ from all the progenitors present at a given redshift. The results for that are shown in the left panel of Fig. 9. The mass on the x-axes of the right panels is the sum of the stellar mass of all progenitors present at that redshift. We here distinguish between field and cluster environment by associating the field with a dark matter halo of 10^{12} $M_\odot$ and the cluster with a dark matter halo of 10^{15} $M_\odot$ at $z = 0$.

For field galaxies at early times ($z > 5$), when the mass in progenitors is still small ($< 10^{10}$ $M_\odot$), gravitational heating is not important. Heating/feedback will be dominantly provided by supernovae and some, if any, AGNs in massive galaxies. At late times gravitational heating is catching up with supernovae. Central and Satellite galaxies in the field are very unlikely to develop strong gravitational heating at any time during their evolution, as a consequence in first approximation it might be justified to neglect these effects when modelling their evolution. However, the situation is dramatically different for cluster galaxies. The central galaxies in these environments, that later become first brightest cluster
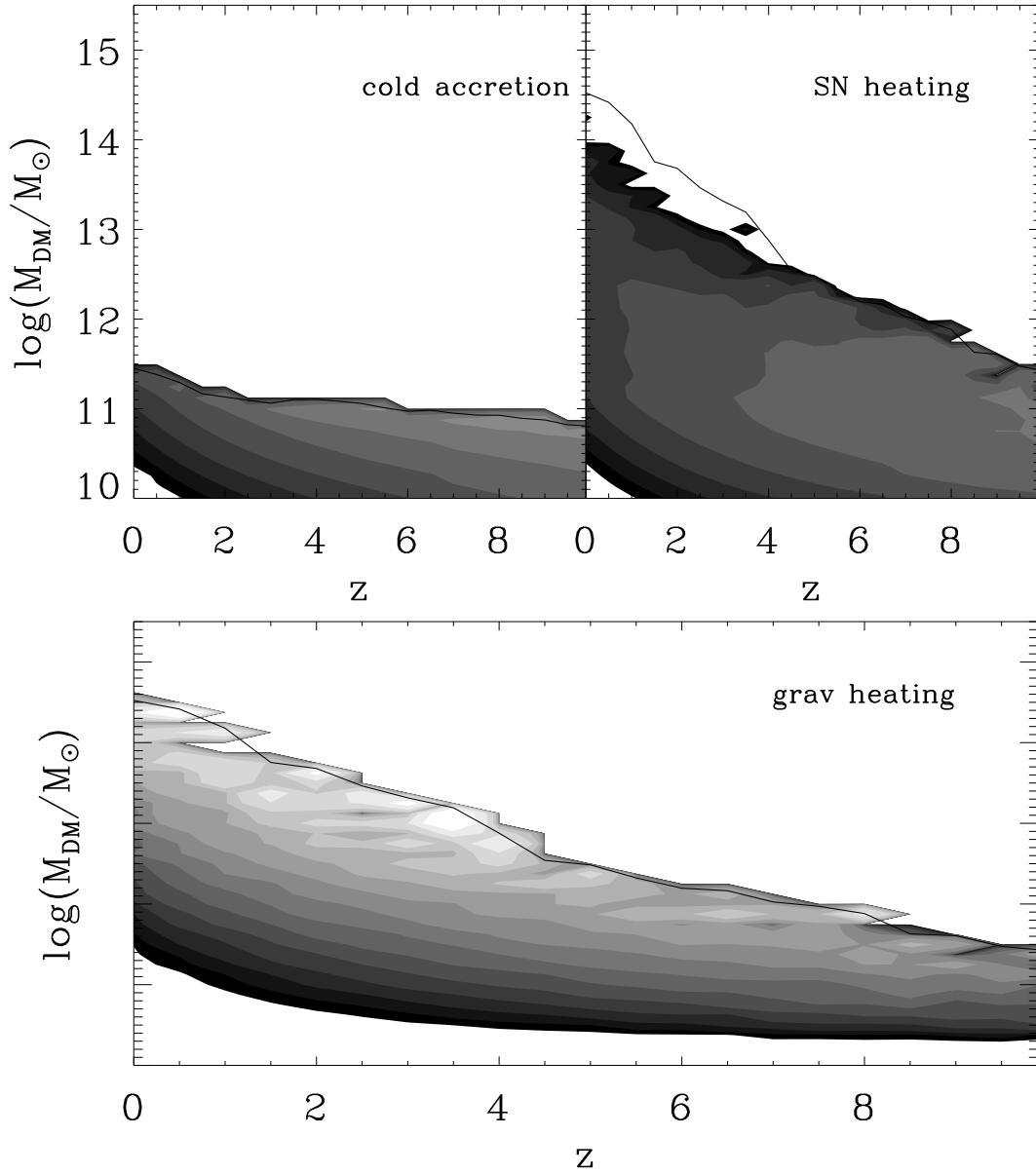
FIG. 8.— The rate of cooling (heating) as a function of dark halo mass and redshift. The solid line in the top left panel shows the maximum halo mass in which cold accretion occurs, while the solid line in the other panels shows the maximum dark halo mass we find at any given redshift. Contours have a factor of two difference from each other. The level of the contours starting with the color black and increasing toward lighter colors are $1, 2, 4, 8...8192$. (

galaxies generally have gravitational heating surpassing supernovae feedback at redshifts around $z = 5$. Present-day cluster member galaxies on the other hand, depending on their mass, will surpass supernovae feedback at later times when their mass is large enough ($> 10^{11}$ M$_\odot$) and stop increasing in ϵ once they become cluster members. It is interesting to note that for the first brightest cluster galaxies gravitational heating steadily increases and continues to become very important at late times and that the overall energy released will exceed that of the AGN but only later when the main AGN activity is already over.

5. COSMIC STAR FORMATION RATE

The observed average cosmic star formation rate (Lilly et al. 1996; Madau et al. 1996) shows a strong de-

cline at redshifts less $z \sim 2$ and a modest decline at $z > 3$ (e.g Giavalisco et al. 2004), a trend generally recovered by semi-analytic models with varying accuracy (e.g. Cole et al. 2000; Giavalisco et al. 2004). One of the occurring problems in these models is the steep decline of the star formation rate at low redshifts while reproducing the star formation rates at high redshifts. Different approaches have shown some progress in that respect by e.g. including feedback form super-massive black holes (e.g. Bower et al. 2006; Croton et al. 2006) which helps reducing star formation in early type galaxies at late times or by the shut off of star formation in halos above a critical mass (Cattaneo et al. 2006).

The environmental effects introduced in the previous sections start operating effectively in high density envi-
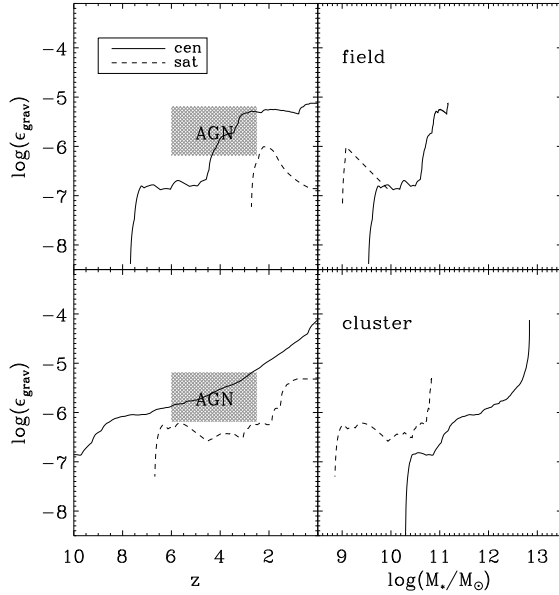
FIG. 9.— The $\epsilon-$trajectory of gravitational heating in field galaxies (top) and cluster galaxies (bottom). We show two set of results for random central galaxies (solid line) and random satellite galaxies (dashed line). We calculate ϵ_{grav} by summing it up over all progenitor galaxies. We do the same for the masses shown on the x-axes of the panels on the right. The shaded area labeled AGN shows the range over which AGN-activity is expected.

ronments like clusters of galaxies and are able to prevent cooling of gas and associated star formation. The average cosmic star formation rate (Lilly et al. 1996; Madau et al. 1996) in that sense provides an ideal way to compare our model predictions and to judge the importance of the effects we added. Our model prediction, shown as the solid line in Fig. 10, is in quite good agreement with the observations summarized by Hopkins (2004). Our new model differs from the best fit initial SAM (dashed line) in one very important point, we find higher star formation rates at $z > 3$ and significantly lower ones at $z < 2$. Furthermore, we have to reduce the energy deposited in the ISM by super-novae as we do have additional environmental heating sources that counter the cooling rate and regulate the star formation. The reason for the change in shape of the cosmic star formation is that the environmental effects operate not like supernovae feedback which is essentially proportional to the star formation rate, but are dependent on the mass of the halo and its assembly time. We find that many galaxies which dominate the star formation rate at redshifts $z > 4$ and that end up in dense environments at $z = 0$ will not yet have assembled in groups and hence gravitational heating will not be significant. Once the assembly starts taking place during the peak of the merger epoch around $z \sim 2$ (Khochfar & Burkert 2001) the environmental effects start to operate and to provide more feedback than the supernovae and as a consequence the star formation rate declines steeper than in a model with only supernovae feedback.

In Fig. 11 we split the contribution to the cosmic star formation rate into different environments according to the host dark matter halo mass. The top panel illustrates nicely the steep decline of the star formation rate in cluster environments compared to field environments, a signature of down-sizing by environment. In the lower
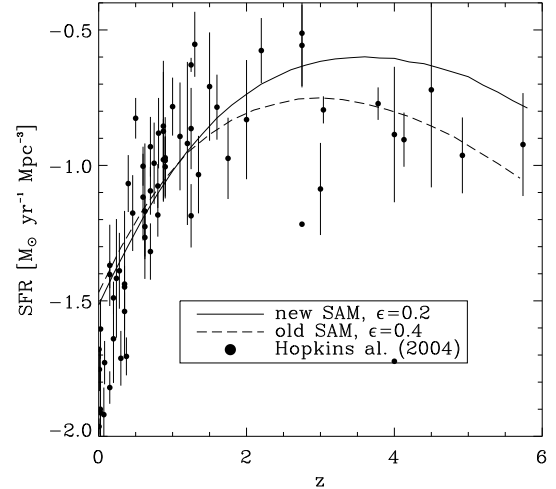

FIG. 10.— Modelled vs observed star formation history. We show the best fit initial SAM (dashed line) and the best fit new model including all environmental effects (solid line). The observed data is the compilation from Hopkins (2004)
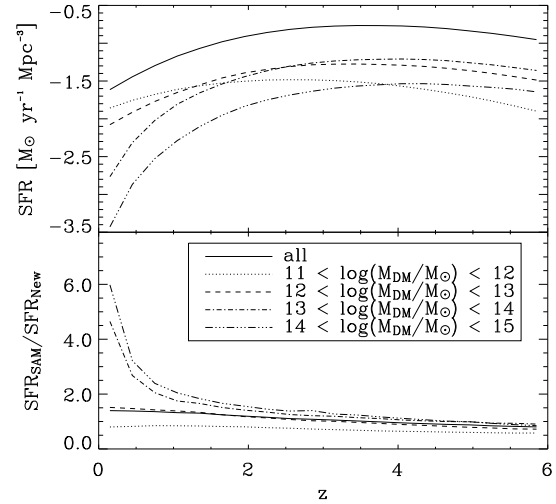

FIG. 11.— Top panel: Cosmic star formation history for the model including all environmental effects. We show results for different environments as indicated by the dark matter halo mass, with larger halo masses representing denser environments. Note how star formation at late times is dominated by low mass galaxies in low density environments. Bottom panel: Ratio of star formation rates in different environments between the initial SAM and the model including the environmental effects using the same supernovae feedback efficiency.

panel we show how the new environmental prescriptions relate to the old SAM prescription with same ϵ. As we mentioned above at low redshifts the star formation is heavily suppressed by up to a factor of six in cluster environments due to our implementation of gravitational heating, while in field environments not much changes. Most of the star formation at late times occurs in low mass systems in moderate density environments.

6. DOWN-SIZING

Growing observational evidence suggests that the main sites of star formation activity changed from massive systems at early times to low mass systems at late times (e.g. Juneau et al. 2005; Thomas et al. 2005; Zheng et al. 2007). A possible explanation for 'down-sizing' from the point of hierarchical modelling is that heating overcomes

cooling at late times in massive systems (Naab et al. 2007). One approach to try to address this problem is e.g. using AGN feedback (Scannapieco et al. 2005; Croton et al. 2006; Bower et al. 2006). We here investigate how environmental effects influence down-sizing. As shown in Figs. 6 & 8 environmental heating is very important for the most massive galaxies and halos. In addition the mass scale affected by environmental heating decreases going to larger redshifts showing down-sizing. It is important to note that we do not claim that these are the sole responsible effects for causing down-sizing but that we investigate their contribution to down-sizing. In Figures 12 & 13 we show the specific star formation rate $\dot{M}_*/M_*$ in units of Gyr^{-1} as a function of the lookback time for galaxies with different present-day masses. Additonally, we split the sample into galaxies residing in massive group/cluster ($M_{DM} > 10^{14}\ \mathrm{M}_\odot$) and field/small group ($M_{DM} < 10^{13}\ \mathrm{M}_\odot$) environments. The results for the best fit old SAM without environmental effects show a long extended tail to low redshifts even for the most massive galaxies, and no strong difference between massive $\log M_* > 11.4$ and low mass galaxies with $\log M_* < 11.4$ (Fig. 12). In addition there is no strong environmental dependence in the specific star formation rate. The new SAM including environmental effects differs in several fundamental ways which are important with respect to down-sizing. First, massive galaxies with $\log M_* > 11.4$ have a strongly peaked star formation epoch at lookback times around 11 Gyrs with a strong decline to smaller lookback times and low mass galaxies with $\log M_* < 11.4$ have only a modest decline showing the same trend as expected from down-sizing. Second, we find a strong environmental dependence in form of galaxies more massive than $\log M_* \sim 11.4$ being extremely rare in the field and low mass galaxies showing more star formation at late times in low dense environments. It is interesting to note that we do not find that galaxies of the same mass are significantly older in high density environments.

7. LUMINOSITY FUNCTION

One attractive point of AGN-feedback is that it helps with the over-cooling problem in SAMs and at the same time helps in fitting the luminosity function at the bright end by limiting the mass of the most massive galaxies in the simulations. We here compare the prediction of our low redshift luminosity function with the SDSS $r-$band luminosity function of Blanton et al. (2003). As shown in Fig. 14 the agreement between the model and the observations is very good over a wide range of luminosities. We over-predict the abundance of very luminous galaxies compared to the SDSS luminosity function, which might not be a problem considering that first brightest cluster galaxies are not properly covered by the SDSS photometry nor are star burst galaxies (ULIRG) having most of their energy output in the far infra-red part of the spectrum. Another reason for finding a few too luminous galaxies is that we follow the merging of galaxies using a simplified model based on dynamical friction which is likely to overpredict the number of mergers for massive galaxies. It has been shown by Springel et al. (2001) that in these cases the luminosity function in clusters shows too many luminous galaxies compared to high resolution simulations that follow the orbits of galaxies in clusters.
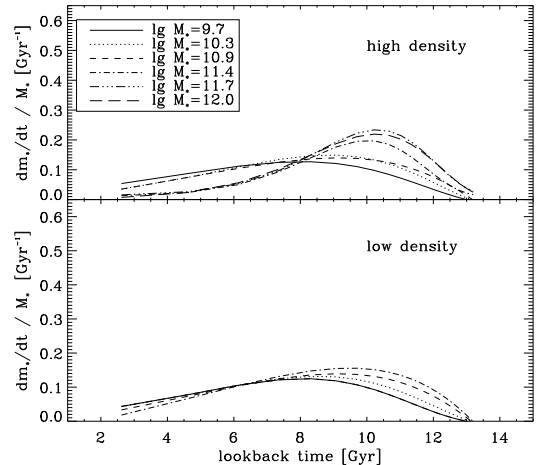

FIG. 12.— The specific star formation rate in units of Gyr^{-1} for galaxies of different present day masses in the old SAM. The upper panel shows only galaxies in cluster environments with $M_{DM} > 10^{14}\ \mathrm{M}_\odot$ and the lower panel only galaxies in field and small group environments with $M_{DM} < 10^{14}\ \mathrm{M}_\odot$. The lines are fits to the simulation data.
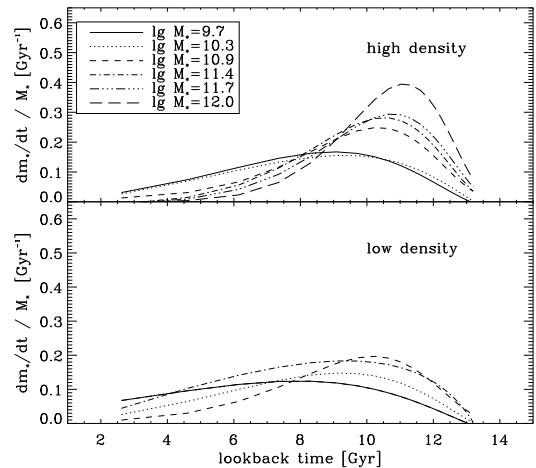

FIG. 13.— Same as Figure 12, but for a SAM including enviormental effects. Note the degree to which low density enviornments dominate at late times.

8. COLOUR-BI-MODALITY

The results by the SDSS (Baldry et al. 2006) or surveys like COMBO-17 (Bell et al. 2004) show that that the galaxy population can be divided according to e.g. its $u - r$-colour into two separate regions with a so-called red-sequence of mostly early-type old non-star forming galaxies and a blue cloud of mainly late-type star forming galaxies. Until recently SAMs have had problems in recovering a strong pronounced bi-modality and only with the inclusion of feedback processes or other cooling shut-off mechanisms could a good agreement to the data be achieved (Cattaneo et al. 2006; Croton et al. 2006; Bower et al. 2006). Although these models are successful in reproducing the overall distribution of colour in the galaxy population, they find different galaxies populat-
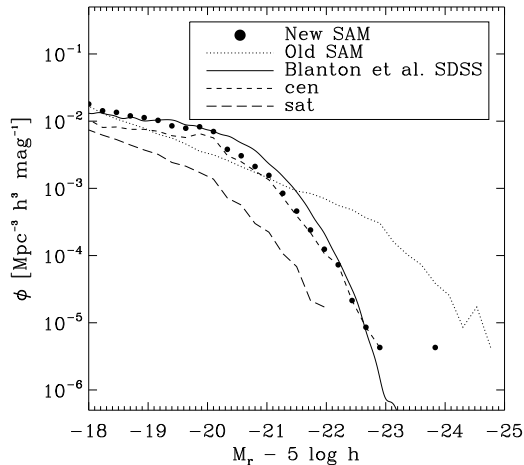
FIG. 14.— Comparison between the $r-$band luminosity function from the SDSS of Blanton et al. (2003) (solid line) and our model predictions (filled black dots). The luminosity function of the central galaxies is shown by the short dashed line and the luminosity function of the satellite galaxies by the long dashed lines. The dotted line shows the predictions of the old SAM with no environmental effects.
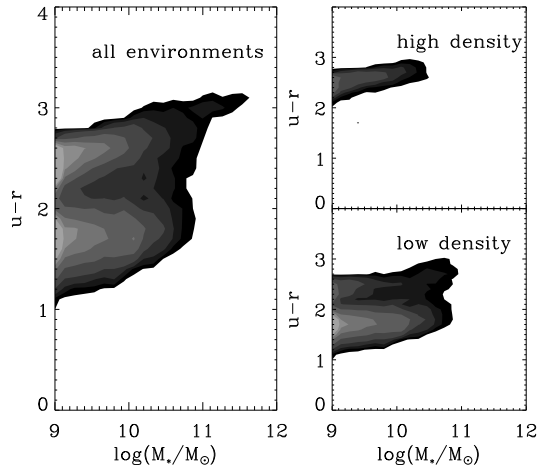

FIG. 15.— The colour-mass relation found in our simulations. Left panel shows the overall distribution and the top and bottom right panel the colour-magnitude relation in high and low-density environments, respectively, using the same environment definition as in Fig. 12.

ing their red-sequence and blue cloud. We here predict the colour distribution of our model galaxies based on the inclusion of the environmental effects. The effect of dust on galaxy colors is estimated using the plane-parallel slab model of Kauffmann et al. (1999). For details of this model we refer the reader to Kauffmann et al. (1999) and to references therein. Fig. 15 shows the colour-mass diagram and it is very clear to see that we produce a very pronounced bi-modality. The low mass part of our red sequence is dominated by satellite galaxies being part of a massive group or cluster environment. This is in agreement with recent findings of Haines et al. (2006). The blue sequence at the low mass end on the other hand is dominated by star forming central galaxies in field environments. At mass $\log M_* > 10.2$ central galaxies start to leave the blue sequence and occupy the red sequence with $u - r > 2.5$. A detailed comparison to the data of Baldry et al. (2006) will be presented in a later paper in which we combine our SAM with a large-scale N-body simulation.

9. DISCUSSION AND CONCLUSIONS

In this paper we presented a first step in including physical effects that are connected to the environment in which galaxies reside into a SAM. Our approach is novel in that we consider how much gravitational potential energy can be released by gas that is stripped from satellite galaxies, once one takes into account the energy needed to strip it. It turns out that this source of gravitational heating is very dependent on the environment, as the amount of potential energy gained for a unit mass coming from infinity increases with the mass of the dark matter halo, which is a good proxy for the density of the environment and we find a scaling with dark matter mass of $\propto M_{DM}^{1.1}$.

Gravitational heating in general is more important for galaxies that reside in environments that can secure a steady infall of gas-rich satellite galaxies, whose stripped gas contributes potential energy. This is naturally the case for present day clusters and massive groups, and

we indeed find in our simulations most of the gravitational heating occurring in these environments. At earlier times the sites of gravitational heating turn to somewhat smaller dark matter halos and hence less dense environments. This is not surprising considering that the mass of 2σ halos, the mass we can associate with massive groups and clusters today, decreases at earlier times. The build up of dark matter on the scales we consider here is approximately self-similar and one would expect roughly as much substructure falling into a 2σ halo at early times as on a 2σ halo at late times. The main difference will be in the higher gas fraction of the infalling satellites at earlier times. The higher gas fraction almost compensates for the lower potential energy per unit mass in the 2σ halos at earlier times causing them to have similar ϵ_{grav} as their counter parts at low redshifts. In this respect our environmental effects are purely driven by the dark matter formation path.

One of the natural outcomes from including gravitational heating is down-sizing (Zheng et al. 2007) in the star-formation rate of massive galaxies. Central galaxies residing in the most dense environments generally have a very significant contribution by gravitational heating with $\epsilon_{grav} \sim 3 \times 10^{-4}$ which is greater than or comparable to the amount of feedback from AGNs (Springel et al. 2005; Ciotti & Ostriker 2007). However, the way that these two heating sources operate is very different. While luminous AGNs will heat most efficient during a QSO-phase that takes place at redshifts $z > 3$ (Hasinger et al. 2005) gravitational heating will start heating more efficiently than AGNs at redshifts $z < 2$. This is connected to the epoch when most massive environments assemble by merging of groups. Besides being effective at late times, gravitational heating has the additional feature of showing a strong mass dependence that can produce the right trend of down-sizing in the star formation rate of galaxies. Low mass galaxies around 10^{11} M$_\odot$ generally have $\epsilon_{grav} \leq \epsilon_{SN}$ and star formation is regulated mainly by supernovae feedback which by itself will not produce down-sizing. Galaxies more massive than that have $\epsilon_{grav} > \epsilon_{SN}$ and star formation will be regulated by

gravitational heating. In summary the following picture emerges, at large redshifts a first episode of strong heating occurs when AGNs have their peak activity. During that phase a great deal of energy will be deposited within the ISM/ICM. After that gravitational heating will start kicking in mainly in the most massive systems regulating the cooling rate of gas and hence the star formation rate. We thus argue that down-sizing at low redshifts is a consequence of the redshift and mass dependence of gravitational heating, which is driven by the environment.

In a study of galaxy properties within the Sloan Digital Sky Survey, Kauffmann et al. (2003) find that galaxy properties show a bimodal distribution around $M_{crit} = 3 \times 10^{10}$ M$_\odot$. Galaxies more massive than this have generally older stellar populations than those less massive. It is an intriguing question to ask what could be the origin for this abrupt transition (see e.g. Dekel & Birnboim 2006). The reason for the transition must be closely related the ability to make stars. One natural suspect in this respect is feedback. The general prime suspect for feedback, supernovae and AGN feedback, do not show a characteristic mass scale at which their action occurs. The energy output per unit stellar mass is independent of the mass of the galaxy for both AGN and SN feedback, but increases as $M_*^{1.2}$ for gravitational heating. However, it should be noted that the effects of a given amount of heating can be scale dependent and hence introduce a characteristic mass scale for supernovae and AGN feedback as well. Additionally we find that gravitational heating shows a distinctive transition at a mass scale of $\sim 3 \times 10^{10}$ M$_\odot$ from being roughly constant at smaller masses to increasing steadily at higher masses. Galaxies below M_{crit} in our simulation are mostly unaffected by gravitational heating and hence their star formation is regulated by supernovae feedback. Above M_{crit} the situation changes when gravitational heating start becoming more important and able to influence star formation by contributing significant amounts of feedback. Even when $\epsilon_{grav} < \epsilon_{SN}$, it will be important as a source of feedback and regulator for star formation, because it operates independently of the star formation in contrast to supernovae feedback, and it will contribute significant amount of heating energy at late times. Again, just as in the case of down-sizing, the feature that could cause the transition mass scale M_{crit} is the specific mass dependency and epoch when gravitational heating kicks in.

It is interesting to make the connection between our work and previous work by Blanton et al. (1999) who suggest a scale dependent bias for the galaxy population, in a sense that massive, red galaxies reside within high density environments. Combining this with results of Nagamine et al. (2006) suggest that one should expect a drop in the star formation rate for present-day massive red galaxies that reside in massive environments, just as we predicted within our model.

In this paper we included gravitational heating effects in our SAM based on simplified physical models and made some first predictions/comparisons. The results so far seem very promising and we will present more detailed comparisons to observations in a follow-up paper. It is clear that this can only be viewed as a first step in trying to include environmental effects and that further comparisons to high resolution hydrodynamical simulations will be necessary to improve on this effort.

REFERENCES

Abadi, M. G., Moore, B., & Bower, R. G. 1999, MNRAS, 308, 947

Baldry, I. K., Balogh, M. L., Bower, R. G., Glazebrook, K., Nichol, R. C., Bamford, S. P., & Budavari, T. 2006, MNRAS, 373, 469

Bell, E. F., et al. 2004, ApJ, 608, 752

Benson, A. J., Lacey, C. G., Baugh, C. M., Cole, S., & Frenk, C. S. 2002, MNRAS, 333, 156

Benson, A. J., Bower, R. G., Frenk, C. S., Lacey, C. G., Baugh, C. M., & Cole, S. 2003, ApJ, 599, 38

Binney, J. 1977, ApJ, 215, 483 p.,

Binney, J. 2004, MNRAS, 347, 1093

Birnboim, Y., & Dekel, A. 2003, MNRAS, 345, 349

Birnboim, Y., Dekel, A., & Neistein, E. 2007, ArXiv Astrophysics e-prints, arXiv:astro-ph/0703435

Blanton, M., Cen, R., Ostriker, J. P., & Strauss, M. A. 1999, ApJ, 522, 590

Blanton, M., Cen, R., Ostriker, J. P., Strauss, M. A., & Tegmark, M. 2000, ApJ, 531, 1

Blanton, M. R., et al. 2003, ApJ, 592, 819

Bower, R. G., Benson, A. J., Malbon, R., Helly, J. C., Frenk, C. S., Baugh, C. M., Cole, S., & Lacey, C. G. 2006, MNRAS, 370, 645

Bryan, G. L., & Norman, M. L. 1998, ApJ, 495, 80

Bullock, J. S., Kolatt, T. S., Sigad, Y., Somerville, R. S., Kravtsov, A. V., Klypin, A. A., Primack, J. R., & Dekel, A. 2001, MNRAS, 321, 559

Butcher, H., & Oemler, A., Jr. 1978, ApJ, 219, 18

Butcher, H., & Oemler, A., Jr. 1984, ApJ, 285, 426

Cattaneo, A., Dekel, A., Devriendt, J., Guiderdoni, B., & Blaizot, J. 2006, MNRAS, 370, 1651

Ciotti, L., & Ostriker, J. P. 2001, ApJ, 551, 131

Ciotti, L., & Ostriker, J. P. 2007, ArXiv Astrophysics e-prints, arXiv:astro-ph/0703057

Cole, S., Lacey, C. G., Baugh, C. M., & Frenk, C. S. 2000, MNRAS, 319, 168 (C00)

Cooper, M. C., et al. 2006, MNRAS, 370, 198

Croton, D. J., et al. 2006, MNRAS, 365, 11

De Lucia, G., & Blaizot, J. 2007, MNRAS, 375, 2

Dekel, A., & Silk, J. 1986, ApJ, 303, 39

Dekel, A., & Birnboim, Y. 2006, MNRAS, 368, 2

Dolag, K., Bartelmann, M., Perrotta, F., Baccigalupi, C., Moscardini, L., Meneghetti, M., & Tormen, G. 2004, A&A, 416, 853

Dressler, A. 1980, ApJ, 236, 351

Dressler, A., & Gunn, J. E. 1982, ApJ, 263, 533

Dressler, A. 1986, ApJ, 301, 35

Farouki, R., & Shapiro, S. L. 1980, ApJ, 241, 928

Frenk, C. S., et al. 1999, ApJ, 525, 554

Giavalisco, M., et al. 2004, ApJ, 600, L103

Giovanelli, R., & Haynes, M. P. 1983, AJ, 88, 881

Gnedin, N. Y. 2000, ApJ, 542, 535

Gunn, J. E., & Gott, J. R. I. 1972, ApJ, 176, 1

Haines, C. P., La Barbera, F., Mercurio, A., Merluzzi, P., & Busarello, G. 2006, ApJ, 647, L21

Hasinger, G., Miyaji, T., & Schmidt, M. 2005, A&A, 441, 417

Hatton, S., Devriendt, J. E. G., Ninin, S., Bouchet, F. R., Guiderdoni, B., & Vibert, D. 2003, MNRAS, 343, 75

Hopkins, A. M. 2004, ApJ, 615, 209

Juneau, S., et al. 2005, ApJ, 619, L135

Kang, X., Jing, Y. P., & Silk, J. 2006, ApJ, 648, 820

Kauffmann, G., Colberg, J. M., Diaferio, A., & White, S. D. M. 1999, MNRAS, 303, 188 (K99)

Kauffmann, G., et al. 2003, MNRAS, 341, 54

Kennicutt, R. C., Jr. 1998, ApJ, 498, 541

Kereš, D., Katz, N., Weinberg, D. H., & Davé, R. 2005, MNRAS, 363, 2

Khochfar, S., & Burkert, A. 2001, ApJ, 561, 517

Khochfar, S., & Burkert, A. 2003, ApJ, 597, L117

Khochfar, S., & Burkert, A. 2005, MNRAS, 359, 1379

Khochfar, S., & Burkert, A. 2006, A&A, 445, 403

Khochfar, S., & Silk, J. 2006a, MNRAS, 370, 902

Khochfar, S., & Silk, J. 2006b, ApJ, 648, L21

Lanzoni, B., Guiderdoni, B., Mamon, G. A., Devriendt, J., & Hatton, S. 2005, MNRAS, 361, 369

Lilly, S. J., Le Fevre, O., Hammer, F., & Crampton, D. 1996, ApJ, 460, L1

Machacek, M., Jones, C., Forman, W. R., & Nulsen, P. 2006, ApJ, 644, 155

Marcillac, D., Rigby, J. R., Rieke, G. H., & Kelly, D. M. 2007, ApJ, 654, 825

Madau, P., Ferguson, H. C., Dickinson, M. E., Giavalisco, M., Steidel, C. C., & Fruchter, A. 1996, MNRAS, 283, 1388

Mayer, L., Moore, B., Quinn, T., Governato, F., & Stadel, J. 2002, MNRAS, 336, 119

Metzler, C. A., & Evrard, A. E. 1994, ApJ, 437, 564

Moran, S. M., Ellis, R. S., Treu, T., Salim, S., Rich, R. M., Smith, G. P., & Kneib, J.-P. 2006, ApJ, 641, L97

Mori, M., & Burkert, A. 2000, ApJ, 538, 559

Naab, T., Johansson, P. H., Ostriker, J. P., & Efstathiou, G. 2007, ApJ, 658, 710

Naab, T., & Ostriker, J. P. 2006, MNRAS, 366, 899

Nagamine, K., Ostriker, J. P., Fukugita, M., & Cen, R. 2006, ApJ, 653, 881

Neistein, E., van den Bosch, F. C., & Dekel, A. 2006, MNRAS, 372, 933

Okamoto, T., & Nagashima, M. 2003, ApJ, 587, 500

Quilis, V., Moore, B., & Bower, R. 2000, Science, 288, 1617

Rees, M. J., & Ostriker, J. P. 1977, MNRAS, 179, 541

Scannapieco, E., Silk, J., & Bouwens, R. 2005, ApJ, 635, L13

Shapiro, P. R., Iliev, I. T., & Raga, A. C. 1999, MNRAS, 307, 203

Silk, J. 1977, ApJ, 211, 638

Shen, S., Mo, H. J., White, S. D. M., Blanton, M. R., Kauffmann, G., Voges, W., Brinkmann, J., & Csabai, I. 2003, MNRAS, 343, 978

Smith, G. P., Treu, T., Ellis, R. S., Moran, S. M., & Dressler, A. 2005, ApJ, 620, 78

Somerville, R. S., & Primack, J. R. 1999, MNRAS, 310, 1087

Somerville, R. S., & Kolatt, T. S. 1999, MNRAS, 305, 1

Somerville, R. S., Lemson, G., Kolatt, T. S., & Dekel, A. 2000, MNRAS, 316, 479

Somerville, R. S. 2002, ApJ, 572, L23

Spergel, D. N., et al. 2007, ApJS, 170, 377

Springel, V., White, S. D. M., Tormen, G., & Kauffmann, G. 2001, MNRAS, 328, 726 (S01)

Springel, V., Di Matteo, T., & Hernquist, L. 2005, ApJ, 620, L79

Sutherland, R. S., & Dopita, M. A. 1993, ApJS, 88, 253

Ostriker, J. P., Bode, P., & Babul, A. 2005, ApJ, 634, 964

Taylor, J. E., & Babul, A. 2001, ApJ, 559, 716

Thomas, D., Maraston, C., Bender, R., & Mendes de Oliveira, C. 2005, ApJ, 621, 673

Trujillo, I., et al. 2005, ArXiv Astrophysics e-prints, arXiv:astro-ph/0504225

van Dokkum, P. G., Franx, M., Fabricant, D., Kelson, D. D., & Illingworth, G. D. 1999, ApJ, 520, L95

van Gorkom, J. H. 2004, Clusters of Galaxies: Probes of Cosmological Structure and Galaxy Evolution, 305

Wang, P., & Abel, T. 2007, ArXiv Astrophysics e-prints, arXiv:astro-ph/0701363

White, S. D. M., & Rees, M. J. 1978, MNRAS, 183, 341

White, S. D. M., & Frenk, C. S. 1991, ApJ, 379, 52 (WF91)

Zheng, X. Z., Bell, E. F., Papovich, C., Wolf, C., Meisenheimer, K., Rix, H.-W., Rieke, G. H., & Somerville, R. 2007, ArXiv Astrophysics e-prints, arXiv:astro-ph/0702208